HAL
open science

v4, v5, v6, v7: nonlinear hydrodynamic response versus LHC data

Li Yan, Jean-Yves Ollitrault

To cite this version:

Li Yan, Jean-Yves Ollitrault. v4, v5, v6, v7: nonlinear hydrodynamic response versus LHC data. Physics Letters B, 2015, 744, pp.82-87. 10.1016/j.physletb.2015.03.040 . cea-01323577

HAL Id: cea-01323577

https://cea.hal.science/cea-01323577

Submitted on 30 May 2016

HAL is a multi-disciplinary open access archive for the deposit and dissemination of scientific research documents, whether they are published or not. The documents may come from teaching and research institutions in France or abroad, or from public or private research centers.

L'archive ouverte pluridisciplinaire **HAL**, est destinée au dépôt et à la diffusion de documents scientifiques de niveau recherche, publiés ou non, émanant des établissements d'enseignement et de recherche français ou étrangers, des laboratoires publics ou privés.

v_4, v_5, v_6, v_7: nonlinear hydrodynamic response versus LHC data

Li Yan[1] and Jean-Yves Ollitrault[1]

[1] *Institut de physique théorique, Université Paris Saclay, CNRS, CEA, F-91191 Gif-sur-Yvette, France*

(Dated: February 10, 2015)

Higher harmonics of anisotropic flow (v_n with $n \geq 4$) in heavy-ion collisions can be measured either with respect to their own plane, or with respect to a plane constructed using lower-order harmonics. We explain how such measurements are related to event-plane correlations. We show that CMS data on v_4 and v_6 are compatible with ATLAS data on event-plane correlations. If one assumes that higher harmonics are the superposition of non-linear and linear responses, then the linear and non-linear parts can be isolated under fairly general assumptions. By combining analyses of higher harmonics with analyses of v_2 and v_3, one can eliminate the uncertainty from initial conditions and define quantities that only involve nonlinear hydrodynamic response coefficients. Experimental data on v_4, v_5 and v_6 are in good agreement with hydrodynamic calculations. We argue that v_7 can be measured with respect to elliptic and triangular flow. We present predictions for v_7 versus centrality in Pb-Pb collisions at the LHC.

PACS numbers: 25.75.Ld, 24.10.Nz

arXiv:1502.02502v1 [nucl-th] 9 Feb 2015

I. INTRODUCTION

In the last year or so, LHC and RHIC experiments have probed anisotropic flow [1] and its fluctuations [2, 3] to an unprecedented degree of precision [4–8]. These new analyses include in particular detailed analyses of higher Fourier harmonics (v_4, v_5, v_6) and their correlations with lower harmonics (v_2, v_3). The scope of this paper is twofold. The first goal is to point out specific relations between seemingly different observables found in the recent experimental literature, and to propose new observables. The second goal is to show that measurements of higher harmonics can be combined with measurements of lower harmonics in a way that facilitates comparison with theory. As an illustration, recent experimental results are compared with hydrodynamic calculations.

The CMS Collaboration has measured v_4 and v_6 with respect to their own direction, and with respect to the direction of elliptic flow v_2 [4] (see also [8]); on the other hand, the ATLAS Collaboration has measured a large number of event-plane correlations [5]. In Sec. II, we clarify the relation between these observables and show how they are related to one another. In particular, we show that CMS and ATLAS data on v_4 and v_6 are compatible. We explain how odd harmonics, such as v_5 or v_7, can also be analyzed with respect to the direction of lower harmonics.

While recent experimental data have been compared to several theoretical models, either event-by-event hydrodynamic calculations [9–12] or tranport models [13], these comparisons offer little insight into the physics of higher-order harmonics. In particular, theoretical calculations depend strongly on the model of the initial density profile, which has long been recognized as the main source of uncertainty in modeling anisotropic flow [14]. On the other hand, there are hints that the physics of higher-order harmonics should be simple: for instance, the ratio $v_4/(v_2)^2$ [15, 16] is equal to $\frac{1}{2}$ at high transverse momentum p_T in ideal hydrodynamics.

In hydrodynamics, higher-order harmonics are superpositions of linear and non-linear response terms [17–20]. This is recalled in Sec. III. We explain how the linear and nonlinear terms can be isolated under fairly general assumptions. We show how analyses of higher-order harmonics can be combined with analyses of lower-order harmonics (v_2 and v_3) to form quantities which do not involve the initial state. These quantities are compared with hydrodynamic calculations.

In Sec. IV, we list a few predictions for higher-order harmonics; in particular, we predict the value of v_7, measured with respect to v_2 and v_3, as a function of centrality.

II. OBSERVABLES FOR HIGHER HARMONICS

Anisotropic flow is an azimuthal (φ) asymmetry of the single-particle distribution [21]:

$$P(\varphi) = \frac{1}{2\pi} \sum_{n=-\infty}^{+\infty} V_n e^{-in\varphi}, \tag{1}$$

where $V_n = v_n \exp(in\Psi_n)$ is the (complex) anisotropic flow coefficient in the nth harmonic, and $V_{-n} = V_n^*$. Both the magnitude [22] and phase [2, 23] of V_n fluctuate event to event.

The simplest observable involving V_n is a plain rms average [24, 25]:

$$v_n\{\Psi_n\} \equiv \sqrt{\langle |V_n|^2 \rangle}, \tag{2}$$

where angular brackets denote an average over events. The notation $v_n\{\Psi_n\}$ has been used earlier to denote the value analyzed with the event-plane method [4]. However, the event-plane method does does not quite measure the rms average [26]. Therefore it should be replaced by the scalar-product method [27], which is recalled in Appendix A. Note that our $v_n\{\Psi_n\}$ is the same quantity as $v_n\{2\}$ in the notation of the cumulant analysis [28].

Alternatively, V_4 can be analyzed with respect to the direction of V_2 [29, 30], and V_6 can be analyzed with respect to the direction of V_2 or that of V_3,

$$v_4\{\Psi_2\} \equiv \frac{\mathrm{Re}\langle V_4 (V_2^*)^2\rangle}{\sqrt{\langle |V_2|^4\rangle}}$$
$$v_6\{\Psi_2\} \equiv \frac{\mathrm{Re}\langle V_6 (V_2^*)^3\rangle}{\sqrt{\langle |V_2|^6\rangle}}$$
$$v_6\{\Psi_3\} \equiv \frac{\mathrm{Re}\langle V_6 (V_3^*)^2\rangle}{\sqrt{\langle |V_3|^4\rangle}}. \quad (3)$$

The triangular inequality implies $|v_4\{\Psi_2\}| \leq v_4\{\Psi_4\}$, $|v_6\{\Psi_2\}| \leq v_6\{\Psi_6\}$, $|v_6\{\Psi_3\}| \leq v_6\{\Psi_6\}$, i.e., v_4 and v_6 are larger when measured with respect to their own plane than with respect to another plane. The ratio of $v_n\{\Psi_m\}$ and $v_n\{\Psi_n\}$ (where n is a multiple of m) can be written as the Pearson correlation coefficient between V_n and $(V_m)^{n/m}$, which we denote by ρ_{mn}:

$$\rho_{24} \equiv \frac{\mathrm{Re}\langle V_4 (V_2^*)^2\rangle}{\sqrt{\langle |V_4|^2\rangle\langle |V_2|^4\rangle}} = \frac{v_4\{\Psi_2\}}{v_4\{\Psi_4\}}$$
$$\rho_{26} \equiv \frac{\mathrm{Re}\langle V_6 (V_2^*)^3\rangle}{\sqrt{\langle |V_6|^2\rangle\langle |V_2|^6\rangle}} = \frac{v_6\{\Psi_2\}}{v_6\{\Psi_6\}}$$
$$\rho_{36} \equiv \frac{\mathrm{Re}\langle V_6 (V_3^*)^2\rangle}{\sqrt{\langle |V_6|^2\rangle\langle |V_3|^4\rangle}} = \frac{v_6\{\Psi_3\}}{v_6\{\Psi_6\}}. \quad (4)$$

The correlations between event planes measured by ATLAS, which are denoted by $\langle\cos(4(\Phi_2-\Phi_4))\rangle_w$, $\langle\cos(6(\Phi_2-\Phi_6))\rangle_w$ and $\langle\cos(6(\Phi_3-\Phi_6))\rangle_w$ in Ref. [5], are *precisely* ρ_{24}, ρ_{26} and ρ_{36} [13, 31]. Note that the terminology "event-plane correlations" applied to such measurements is somewhat misleading, in the sense that these observables involve not only the angles of V_n, but also their magnitudes [27].

Figure 1 presents a test of the first two lines of Eq. (4), where the left-hand side uses ATLAS data and the right-hand side CMS data. The overall agreement is very good, which shows that CMS and ATLAS data are compatible, even though they are measured with different cuts of tranverse momentum p_T. Note that CMS uses the event-plane method, instead of the scalar-product method. This method yields a slightly lower correlation when the resolution is large [5]. This explains, at least qualitatively, why CMS data are slightly lower than ATLAS data for midcentral collisions in Fig. 1 (a).

While Pearson correlation coefficients are typically analyzed by integrating over all particles in a reference detector [5], analyses of v_n with respect to a specific direction (either Ψ_2 or Ψ_n) can be done differentially, as a function of transverse momentum p_T [30] (see Appendix A for analysis details). Hydrodynamics predicts a slightly different p_T dependence depending on the reference direction [18]. It is therefore interesting to generalize Eq. (3) to odd harmonics. V_5 and V_7 can be analyzed with respect to the directions of V_2 and V_3 in the following way:

$$v_5\{\Psi_{23}\} \equiv \frac{\mathrm{Re}\langle V_5 V_2^* V_3^*\rangle}{\sqrt{\langle |V_2|^2|V_3|^2\rangle}}$$

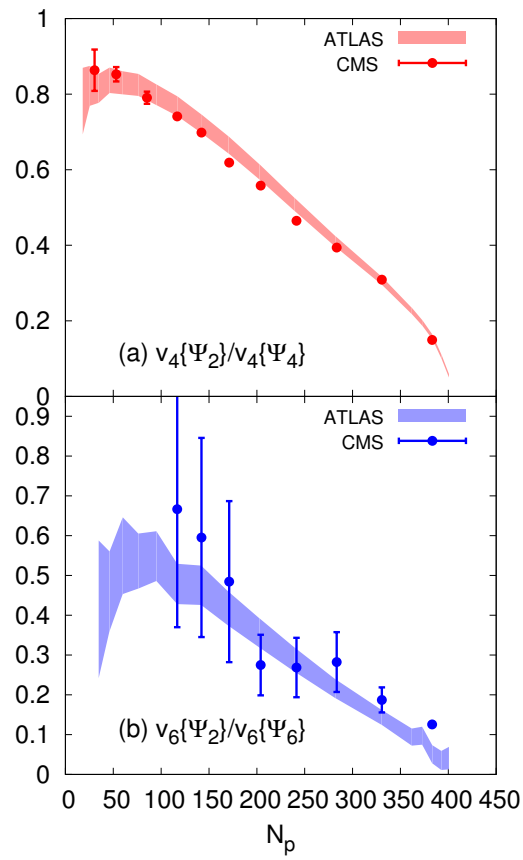

FIG. 1. (Color online) Test of Eqs. (4). Shaded bands correspond to the left-hand side measured by ATLAS [5] in Pb-Pb collisions at 2.76 TeV. Full circles correspond to the right-hand side, obtained using CMS data [4].

$$v_7\{\Psi_{23}\} \equiv \frac{\mathrm{Re}\langle V_7 (V_2^*)^2 V_3^*\rangle}{\sqrt{\langle |V_2|^4|V_3|^2\rangle}}. \quad (5)$$

Quantitative predictions for these quantities will be presented in Sec. IV. These projected harmonics are smaller than those defined by Eq.(2), namely, $|v_5\{\Psi_{23}\}| \leq v_5\{\Psi_5\}$, (and $|v_7\{\Psi_{23}\}| \leq v_7\{\Psi_7\}$). The ratio of $|v_5\{\Psi_{23}\}|$ and $v_5\{\Psi_5\}$ is again the Pearson correlation coefficient between V_5 and V_2V_3:

$$\rho_{23,5} \equiv \frac{\mathrm{Re}\langle V_5 V_2^* V_3^*\rangle}{\sqrt{\langle |V_2|^2|V_3|^2\rangle\langle |V_5|^2\rangle}} = \frac{v_5\{\Psi_{23}\}}{v_5\{\Psi_5\}}. \quad (6)$$

This quantity is very similar to the corresponding three-plane correlation measured by ATLAS [5]:

$$\langle\cos(2\Phi_2+3\Phi_3-5\Phi_5)\rangle_w \equiv \frac{\mathrm{Re}\langle V_5 V_2^* V_3^*\rangle}{\sqrt{\langle |V_2|^2\rangle\langle |V_3|^2\rangle\langle |V_5|^2\rangle}}. \quad (7)$$

More precisely, they coincide if the magnitudes of V_2 and V_3 are uncorrelated,[1] namely, $\langle |V_2|^2|V_3|^2\rangle =$

[1] A slight anticorrelation between $|V_2|^2$ and $|V_3|^2$ has been pre-

$\langle|V_2|^2\rangle\langle|V_3|^2\rangle$. Throughout this paper, we use $\langle\cos(2\Phi_2+3\Phi_3-5\Phi_5)\rangle_w$ from ATLAS as an approximation for ρ_{235}.

Note that even though $v_4\{\Psi_2\}$ and $v_6\{\Psi_2\}$ are smaller than $v_4\{\Psi_4\}$ and $v_6\{\Psi_6\}$, respectively, they are measured with better relative precision [4]. The reason is that these measurements use elliptic flow as a reference, which is measured very accurately. Triangular flow, v_3, is also precisely known. We therefore expect that $v_5\{\Psi_{23}\}$ be determined with better relative accuracy than $v_5\{\Psi_5\}$. In the same way, we expect that even though no experiment has yet been able to detect a nonzero $v_7\{\Psi_7\}$, LHC experiments could already measure $v_7\{\Psi_{23}\}$.

III. LINEAR AND NONLINEAR RESPONSE

In hydrodynamics, anisotropic flow is the response to anisotropy in the initial density profile [34]. Harmonics V_4 and higher can arise from initial anisotropies in the same harmonic [3, 35–37] (linear response) or can be induced by lower-order harmonics [15, 38, 39] (nonlinear response). To a good approximation [20], one can write

$$\begin{aligned} V_4 &= V_{4L} + \chi_4 (V_2)^2 \\ V_5 &= V_{5L} + \chi_5 V_2 V_3 \\ V_6 &= V_{6L} + \chi_{62}(V_2)^3 + \chi_{63}(V_3)^2 \\ V_7 &= V_{7L} + \chi_7 (V_2)^2 V_3, \end{aligned} \tag{8}$$

where V_{nL} denotes the part of V_n due to linear response, and we have included the nonlinear terms involving the largest flow harmonics, V_2 and V_3. The interest of this decomposition is that the nonlinear response coefficients χ are independent of the initial density profile in a given centrality class [18]. We now explain how the linear and nonlinear parts can be isolated.

A. Linear response

The linear part of v_4 and v_5 can be isolated [40] by combining the observables introduced in Sec. II. Using Eqs. (2) and (3), one obtains

$$\begin{aligned} (v_4\{\Psi_4\})^2 - (v_4\{\Psi_2\})^2 &= \langle|V_{4L}|^2\rangle - \frac{|\langle V_{4L}(V_2^*)^2\rangle|^2}{\langle|V_2|^4\rangle} \\ (v_5\{\Psi_5\})^2 - (v_5\{\Psi_{23}\})^2 &= \langle|V_{5L}|^2\rangle - \frac{|\langle V_{5L}V_2^*V_3^*\rangle|^2}{\langle|V_2|^2|V_3|^2\rangle} \end{aligned} \tag{9}$$

These results are general: these combinations always subtract the nonlinear response.

From now on, we further assume that the terms appearing in the right-hand side of Eq. (8) are uncorrelated. That is, we neglect the small correlation between the linear and nonlinear parts which is seen in Monte-Carlo Glauber simulations [18]. The idea behind this assumption is that V_{4L} is produced by initial fluctuations in the fourth harmonic, which are not correlated with the mean eccentricity. Then, the last term in the right-hand side of Eq. (9) vanishes, and the rms value of the linear part is

$$\begin{aligned} v_{4L} &\equiv \sqrt{\langle|V_{4L}|^2\rangle} = \sqrt{(v_4\{\Psi_4\})^2 - (v_4\{\Psi_2\})^2} \\ v_{5L} &\equiv \sqrt{\langle|V_{5L}|^2\rangle} = \sqrt{(v_5\{\Psi_5\})^2 - (v_5\{\Psi_{23}\})^2}. \end{aligned} \tag{10}$$

This quantity has been measured as a function of centrality by the ATLAS collaboration [40].

B. Nonlinear response

The nonlinear parts are obtained by projecting Eq. (8) onto lower harmonics. Assuming again that the terms in the right-hand side of Eq. (8) are uncorrelated, one obtains the following expressions for nonlinear response coefficients:

$$\begin{aligned} \chi_4 &= \frac{\langle V_4(V_2^*)^2\rangle}{\langle|V_2|^4\rangle} = \frac{v_4\{\Psi_2\}}{\sqrt{\langle|V_2|^4\rangle}} \\ \chi_5 &= \frac{\langle V_5 V_2^* V_3^*\rangle}{\langle|V_2|^2|V_3^2|\rangle} = \frac{v_5\{\Psi_{23}\}}{\sqrt{\langle|V_2|^2|V_3^2|\rangle}} \\ \chi_{62} &= \frac{\langle V_6(V_2^*)^3\rangle}{\langle|V_2|^6\rangle} = \frac{v_6\{\Psi_2\}}{\sqrt{\langle|V_2|^6\rangle}} \\ \chi_{63} &= \frac{\langle V_6(V_3^*)^2\rangle}{\langle|V_3|^4\rangle} = \frac{v_6\{\Psi_3\}}{\sqrt{\langle|V_3|^4\rangle}} \\ \chi_7 &= \frac{\langle V_7(V_2^*)^2 V_3^*\rangle}{\langle|V_2|^4|V_3^2|\rangle} = \frac{v_7\{\Psi_{23}\}}{\sqrt{\langle|V_2|^4|V_3^2|\rangle}}. \end{aligned} \tag{11}$$

The left-hand side of these expressions can be calculated in hydrodynamics, and is independent of the model of initial conditions, while the right-hand side can be inferred from experimental data. Eq. (11) therefore offers a direct comparison between hydrodynamics and data, where all dependence on initial state is eliminated [41]. Nonlinear response coefficients have been obtained using event-shape engineering [40] by the ATLAS collaboration. The present method does not require event-shape engineering. The comparison between hydrodynamics and data is shown in Fig. 2, and we now explain in detail how these results are obtained.

The numerators in the right-hand side of Eq. (11) are the projected harmonics defined by Eqs. (3) and (5). We use $v_4\{\Psi_2\}$ and $v_6\{\Psi_2\}$ measured by CMS [4].[2] $v_5\{\Psi_{23}\}$ and $v_6\{\Psi_3\}$ are not measured directly, but can be inferred from $v_5\{\Psi_5\}$, $v_6\{\Psi_6\}$, ρ_{235} and ρ_{36} using Eqs. (4) and (6). We use CMS data [4] for $v_5\{\Psi_5\}$ and $v_6\{\Psi_6\}$ and ATLAS data [5] for ρ_{235} and ρ_{36}. These correlation coefficients, however, are expected to depend little on the experimental setup, as illustrated in Fig. 1.

dicted in AMPT simulations [31–33], but it is at most at the 10% level.

[2] Since CMS uses the event-plane method, the results are slightly lower than the nominal quantities in Eqs. (3) [27].

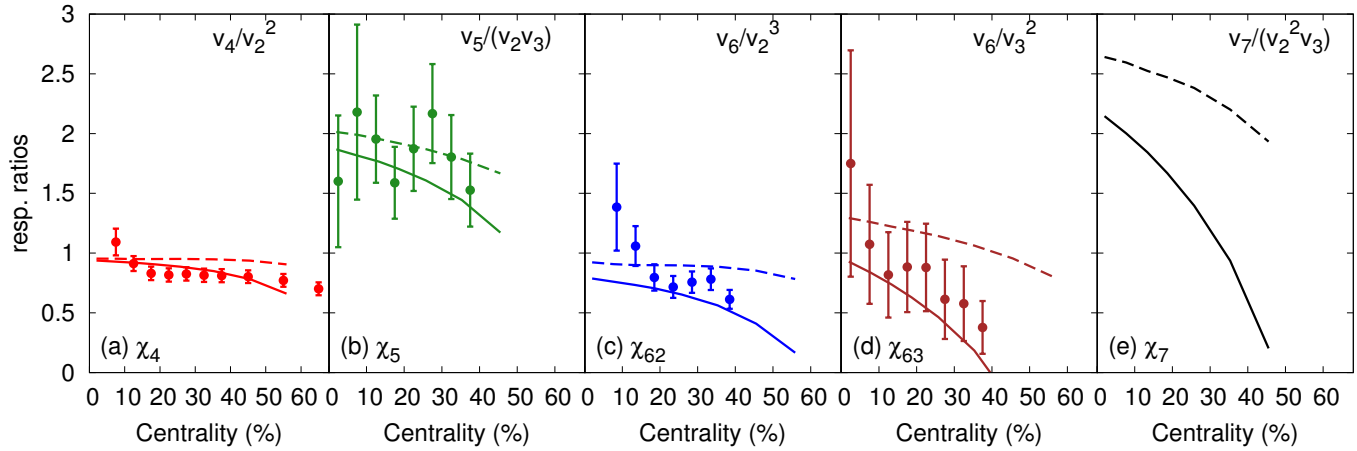

FIG. 2. (Color online) Nonlinear response coefficients defined by Eq. (11) as a function of centrality. Each panel corresponds to a different line of Eq. (11). Dashed lines: ideal hydrodynamics. Solid lines: viscous hydrodynamics with $\eta/s = 0.08$. Symbols: experimental data (see text for details).

The denominators in the right-hand side of Eq. (11) involve various even moments of the distribution of V_2 and V_3. There is no direct measurement of these moments to date. A straightforward procedure to analyze them is outlined in Ref. [31]. Alternatively, moments of the form $\langle |V_n|^{2k} \rangle$ can be inferred from cumulants [28]. The expressions of the first moments in terms of cumulants are:

$$\begin{aligned} \langle |V_n|^2 \rangle &= v_2\{2\}^2 \\ \langle |V_n|^4 \rangle &= 2v_2\{2\}^4 - v_2\{4\}^4 \\ \langle |V_n|^6 \rangle &= 4v_n\{6\}^6 - 9v_n\{4\}^4 v_n\{2\}^2 + 6v_n\{2\}^6. \end{aligned} \quad (12)$$

For the moments involving both V_2 and V_3 (second and fourth line of Eq. (11)), we further assume that the magnitudes of V_2 and V_3 are uncorrelated.

Since different experiments have different acceptance (in particular in transverse momentum p_T), it is important to use results from the same experiment in evaluating the right-hand side of Eq. (11). We use cumulant results from CMS [4]. CMS has not published $v_2\{6\}$, but ATLAS has observed [7] that $v_2\{6\} \simeq v_2\{4\}$ for all centralities, therefore we assume $v_2\{6\} = v_2\{4\}$.

The response coefficients in the left-hand side of Eq. (11) are calculated using hydrodynamics. The calculation shown in Fig. 2 is the same as in Ref. [18]. It uses as initial condition a symmetric Gaussian density profile, where the normalization is adjusted to fit the measured multiplicity dN_{ch}/dy of Pb-Pb collisions at the LHC in the corresponding centrality class. This symmetric profile is deformed in order to produce anisotropic flow in the desired harmonic.[3] We assume uniform longitudinal expansion [42]. With these initial conditions, we solve ideal hydrodynamics or second order viscous hydrodynamics [43] with constant shear viscosity over entropy ratio $\eta/s = 0.08$ [44]. The equation of state is taken from Lattice QCD [45]. The initial time of the calculation is $\tau_o = 1$ fm/c and the freeze-out temperature [46] is $T_{fo} = 150$ MeV. Anisotropic flow, v_n, is calculated at freeze-out. It is averaged over particles in the interval $p_T > 0.3$ GeV/c, corresponding to the CMS acceptance [4].

Figure 2 shows that hydrodynamics naturally captures the sign, the magnitude, and the centrality dependence of all four nonlinear response coefficients. Experimental results differ from hydrodynamic calculations only for the most central bins [41], where the linear part typically becomes larger than the nonlinear part and their correlation can no longer be neglected.

The order of magnitude of the hydrodynamic result can be understood simply. At fixed, large p_T, ideal hydrodynamics predicts [15, 18] $\chi_4 = \frac{1}{2}$, $\chi_5 = 1$, $\chi_{62} = \frac{1}{6}$, $\chi_{63} = \frac{1}{2}$, $\chi_7 = \frac{1}{2}$. However, after averaging over p_T, χ_4 is multiplied by $\langle v_2^2 \rangle / \langle v_2 \rangle^2 > 1$, where brackets now denote an average over p_T in a single hydro event. This is the reason why the results shown in Fig. 2 are larger than the fixed-p_T prediction. Since v_2 and v_3 have similar p_T dependences, the enhancement factor is roughly the same for all quadratic response terms: panels (a), (b), (d) show that $\chi_5 \sim 2\chi_4$, $\chi_{63} \sim \chi_4$, in agreement with the above values. The enhancement from averaging over p_T is larger for cubic response terms than for quadratic terms, but it is similar for both cubic terms: panels (c) and (e) show that $\chi_7 \sim 3\chi_{62}$, also in agreement with the above values.

A full hydrodynamical calculation gives results which differ somewhat from the naive predictions above. Coefficients from ideal hydrodynamics have a slight centrality dependence which is not captured by these formulas [47]. Viscous hydrodynamics predicts lower coefficients than

[3] For instance, χ_4 is obtained by introducing an elliptic deformation and calculating $\chi_4 = v_4/(v_2)^2$.

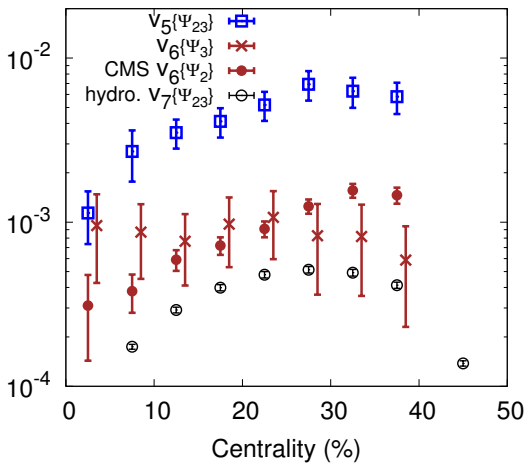

FIG. 3. (Color online) $v_5\{\Psi_{23}\}$, $v_6\{\Psi_2\}$, $v_6\{\Psi_3\}$ and $v_7\{\Psi_{23}\}$, averaged over charged particles with $p_T > 0.3$ GeV/c, as a function of centrality in Pb-Pb collisions at 2.76 TeV. $v_6\{\Psi_3\}$ has been shifted to the right by 1% for sake of clarity.

ideal hydrodynamics. Effect of viscosity, however, cancel to a large extent in the ratios: they are much smaller on $\chi_4 = v_4/(v_2)^2$ than on v_4 and $(v_2)^2$ individually [18].

Nonlinear response coefficients are mostly determined at freeze-out [18], which is probably the least understood part of hydrodynamic calculations. While they depend little on the details of the initial profile or of the hydrodynamic evolution, they depend rather strongly on the freeze-out temperature [47]. Similarly, the dependence of our results on viscosity is mostly through the viscous correction to the momentum distribution at freeze-out [48]. The momentum distribution at freeze-out is not constrained theoretically [49, 50], and the quadratic ansatz used in this calculation is not favored by previous studies of v_4 [51]. Our calculation does not involve bulk viscosity, which is likely to be important at freeze-out [52–55]. Finally, our results are quite sensitive to the value of the freeze-out temperature. Further studies are needed in order to pin down the sensitivity of response coefficients to model parameters.

IV. PREDICTIONS

Figure 3 displays $v_5\{\Psi_{23}\}$, $v_6\{\Psi_2\}$, $v_6\{\Psi_3\}$ and $v_7\{\Psi_{23}\}$. Out of these four quantities, only $v_6\{\Psi_2\}$ has been measured by CMS [4]. We predict $v_5\{\Psi_{23}\}$ and $v_6\{\Psi_3\}$ using Eqs. (4) and (6), where we take $v_5\{\Psi_5\}$ and $v_6\{\Psi_6\}$ from CMS [4] and ρ_{235} and ρ_{36} from ATLAS [5].

Finally, $v_7\{\Psi_{23}\}$ is obtained from the last line of Eq. (11). We use the viscous hydrodynamic calculation for χ_7 shown in Fig. 2 (e). We again assume that the magnitudes of V_2 and V_3 are independent, that is, $\langle |V_2|^4 |V_3^2| \rangle \simeq \langle |V_2|^4 \rangle \langle |V_3^2| \rangle$, and we estimate the moments using Eq. (12) and CMS data [4]. We anticipate that the absolute experimental error on $v_7\{\Psi_{23}\}$ should be similar to the error on $v_6\{\Psi_2\}$. This error is of the order of 0.01%. The predicted values of $v_7\{\Psi_{23}\}$ is 0.05% in the 25-30% centrality range, larger than the error. We therefore expect that a nontrivial $v_7\{\Psi_{23}\}$ could be measured in midcentral Pb-Pb collisions at the LHC.

V. CONCLUSION

Harmonics v_4 and higher can be measured either with respect to their own planes or with respect to lower harmonic planes. We have clarified the relation between these projected harmonics and the so-called event-plane correlations.

We have shown that under fairly general assumptions, measurements of higher harmonics can be combined with measurements of v_2 and v_3 in a way that eliminates the dependence on the initial state, and can be directly compared with hydrodynamic calculations. Experimental results for v_4, v_5 and v_6 are in good agreement with viscous hydrodynamic calculations. We have argued that v_7 could be measured, and presented quantitative predictions.

On the experimental side, analyses should be repeated using the scalar-product method, whose result may differ significantly from the event-plane method for higher harmonics [27]. On the theoretical side, we hope that studies of higher harmonics will help constrain the theoretical description of the fluid close the freeze-out temperature, which is poorly understood at present.

ACKNOWLEDGMENTS

LY is funded by the European Research Council under the Advanced Investigator Grant ERC-AD-267258.

Appendix A: Analysis

The flow observables in Eq. (2), (3) and (5) are expressed in terms of moments of the distribution of V_n. A generic moment is of the form [31]

$$\mathcal{M} \equiv \left\langle \prod_n (V_n)^{k_n} (V_n^*)^{l_n} \right\rangle, \tag{A1}$$

where k_n and l_n are integers and azimuthal symmetry implies $\sum_n n k_n = \sum_n n l_n$. For instance, $\langle V_4 (V_2^*)^2 \rangle$ corresponds to $k_4 = 1$, $l_2 = 2$; $\langle |V_2|^6 \rangle$ corresponds to $k_2 = l_2 = 3$; $\langle |V_2|^4 |V_3|^2 \rangle$ corresponds to $k_2 = l_2 = 2$, $k_3 = l_3 = 1$.

We now describe a simple procedure for measuring these moments [31], which generalizes the scalar-product

method [56]. We define in each collision the flow vector by

$$Q_n \equiv \frac{1}{N}\sum_j e^{in\varphi_j}, \tag{A2}$$

where the sum runs over N particles seen in a reference detector, and φ_j are their azimuthal angles. One measures Q_n in two different parts of the detector ("subevents") A and B, which are symmetric around midrapidity and separated by a gap in pseudorapidity in order to suppress nonflow correlations [13, 57, 58]. The moment (A1) is then given by

$$\mathcal{M} = \left\langle \prod_n (Q_{nA})^{k_n} (Q^*_{nB})^{l_n} \right\rangle. \tag{A3}$$

Applied to Eq. (5), this gives:

$$v_5\{\Psi_{23}\} \equiv \frac{\mathrm{Re}\langle Q_{5A} Q^*_{2B} Q^*_{3B}\rangle}{\sqrt{\mathrm{Re}\langle Q_{2A} Q_{3A} Q^*_{2B} Q^*_{3B}\rangle}}. \tag{A4}$$

The scalar-product method thus uses the magnitude of the flow vector [56] while the traditional event-plane method [59] only uses its azimuthal angle. One can symmetrize the numerator of Eq. (A4) over A and B to decrease the statistical error. Instead of 2 symmetric subevents, one can use 3 non-symmetric subevents, as described in Ref. [27].

Finally, analyses can be done differentially (in p_T bins, for identified particles, etc.). For the differential analysis, one replaces Eq. (A4) by:

$$v_5\{\Psi_{23}\} \equiv \frac{\mathrm{Re}\langle e^{5i\varphi} Q^*_{2B} Q^*_{3B}\rangle}{\sqrt{\mathrm{Re}\langle Q_{2A} Q_{3A} Q^*_{2B} Q^*_{3B}\rangle}}, \tag{A5}$$

where the average in the numerator is now an average over particles in the considered bin, with azimuthal angle φ, instead of an average over events.

[1] U. Heinz and R. Snellings, Ann. Rev. Nucl. Part. Sci. **63**, 123 (2013) [arXiv:1301.2826 [nucl-th]].
[2] B. Alver *et al.* [PHOBOS Collaboration], Phys. Rev. Lett. **98**, 242302 (2007) [nucl-ex/0610037].
[3] B. Alver and G. Roland, Phys. Rev. C **81**, 054905 (2010) [Erratum-ibid. C **82**, 039903 (2010)] [arXiv:1003.0194 [nucl-th]].
[4] S. Chatrchyan *et al.* [CMS Collaboration], Phys. Rev. C **89**, no. 4, 044906 (2014) [arXiv:1310.8651 [nucl-ex]].
[5] G. Aad *et al.* [ATLAS Collaboration], Phys. Rev. C **90**, no. 2, 024905 (2014) [arXiv:1403.0489 [hep-ex]].
[6] B. B. Abelev *et al.* [ALICE Collaboration], Phys. Rev. C **90**, no. 5, 054901 (2014) [arXiv:1406.2474 [nucl-ex]].
[7] G. Aad *et al.* [ATLAS Collaboration], Eur. Phys. J. C **74**, no. 11, 3157 (2014) [arXiv:1408.4342 [hep-ex]].
[8] A. Adare *et al.* [PHENIX Collaboration], arXiv:1412.1038 [nucl-ex].
[9] B. Schenke, S. Jeon and C. Gale, Phys. Rev. C **85**, 024901 (2012) [arXiv:1109.6289 [hep-ph]].
[10] F. G. Gardim, F. Grassi, M. Luzum and J. Y. Ollitrault, Phys. Rev. Lett. **109**, 202302 (2012) [arXiv:1203.2882 [nucl-th]].
[11] Z. Qiu and U. Heinz, Phys. Lett. B **717**, 261 (2012) [arXiv:1208.1200 [nucl-th]].
[12] S. Ryu, J.-F. Paquet, C. Shen, G. S. Denicol, B. Schenke, S. Jeon and C. Gale, arXiv:1502.01675 [nucl-th].
[13] R. S. Bhalerao, J. Y. Ollitrault and S. Pal, Phys. Rev. C **88**, 024909 (2013) [arXiv:1307.0980 [nucl-th]].
[14] M. Luzum and P. Romatschke, Phys. Rev. C **78**, 034915 (2008) [Erratum-ibid. C **79**, 039903 (2009)] [arXiv:0804.4015 [nucl-th]].
[15] N. Borghini and J. Y. Ollitrault, Phys. Lett. B **642**, 227 (2006) [nucl-th/0506045].
[16] C. Lang and N. Borghini, Eur. Phys. J. C **74**, 2955 (2014) [arXiv:1312.7763 [nucl-th]].
[17] F. G. Gardim, F. Grassi, M. Luzum and J. Y. Ollitrault, Phys. Rev. C **85**, 024908 (2012) [arXiv:1111.6538 [nucl-th]].
[18] D. Teaney and L. Yan, Phys. Rev. C **86**, 044908 (2012) [arXiv:1206.1905 [nucl-th]].
[19] D. Teaney and L. Yan, Phys. Rev. C **90**, no. 2, 024902 (2014) [arXiv:1312.3689 [nucl-th]].
[20] F. G. Gardim, J. Noronha-Hostler, M. Luzum and F. Grassi, arXiv:1411.2574 [nucl-th].
[21] M. Luzum, J. Phys. G **38**, 124026 (2011) [arXiv:1107.0592 [nucl-th]].
[22] M. Miller and R. Snellings, nucl-ex/0312008.
[23] R. Andrade, F. Grassi, Y. Hama, T. Kodama and O. Socolowski, Jr., Phys. Rev. Lett. **97**, 202302 (2006) [nucl-th/0608067].
[24] K. Aamodt *et al.* [ALICE Collaboration], Phys. Rev. Lett. **107**, 032301 (2011) [arXiv:1105.3865 [nucl-ex]].
[25] A. Adare *et al.* [PHENIX Collaboration], Phys. Rev. Lett. **107**, 252301 (2011) [arXiv:1105.3928 [nucl-ex]].
[26] B. Alver, B. B. Back, M. D. Baker, M. Ballintijn, D. S. Barton, R. R. Betts, R. Bindel and W. Busza *et al.*, Phys. Rev. C **77**, 014906 (2008) [arXiv:0711.3724 [nucl-ex]].
[27] M. Luzum and J. Y. Ollitrault, Phys. Rev. C **87**, no. 4, 044907 (2013) [arXiv:1209.2323 [nucl-ex]].
[28] N. Borghini, P. M. Dinh and J. Y. Ollitrault, Phys. Rev. C **64**, 054901 (2001) [nucl-th/0105040].
[29] J. Adams *et al.* [STAR Collaboration], Phys. Rev. Lett. **92**, 062301 (2004) [nucl-ex/0310029].
[30] A. Adare *et al.* [PHENIX Collaboration], Phys. Rev. Lett. **105**, 062301 (2010) [arXiv:1003.5586 [nucl-ex]].
[31] R. S. Bhalerao, J. Y. Ollitrault and S. Pal, Phys. Lett. B **742**, 94 (2015) [arXiv:1411.5160 [nucl-th]].
[32] P. Huo, J. Jia and S. Mohapatra, Phys. Rev. C **90**, no. 2, 024910 (2014) [arXiv:1311.7091 [nucl-ex]].

[33] A. Bilandzic, C. H. Christensen, K. Gulbrandsen, A. Hansen and Y. Zhou, Phys. Rev. C **89**, no. 6, 064904 (2014) [arXiv:1312.3572 [nucl-ex]].

[34] S. Floerchinger, U. A. Wiedemann, A. Beraudo, L. Del Zanna, G. Inghirami and V. Rolando, Phys. Lett. B **735**, 305 (2014) [arXiv:1312.5482 [hep-ph]].

[35] D. Teaney and L. Yan, Phys. Rev. C **83**, 064904 (2011) [arXiv:1010.1876 [nucl-th]].

[36] S. S. Gubser and A. Yarom, Nucl. Phys. B **846**, 469 (2011) [arXiv:1012.1314 [hep-th]].

[37] Y. Hatta, J. Noronha, G. Torrieri and B. W. Xiao, Phys. Rev. D **90**, no. 7, 074026 (2014) [arXiv:1407.5952 [hep-ph]].

[38] L. V. Bravina *et al.*, Eur. Phys. J. C **74**, no. 3, 2807 (2014) [arXiv:1311.7054 [nucl-th]].

[39] L. V. Bravina *et al.*, Phys. Rev. C **89**, no. 2, 024909 (2014) [arXiv:1311.0747 [hep-ph]].

[40] J. Jia, J. Phys. G **41**, no. 12, 124003 (2014) [arXiv:1407.6057 [nucl-ex]].

[41] C. Gombeaud and J. Y. Ollitrault, Phys. Rev. C **81**, 014901 (2010) [arXiv:0907.4664 [nucl-th]].

[42] J. D. Bjorken, Phys. Rev. D **27**, 140 (1983).

[43] R. Baier, P. Romatschke, D. T. Son, A. O. Starinets and M. A. Stephanov, JHEP **0804**, 100 (2008) [arXiv:0712.2451 [hep-th]].

[44] P. Kovtun, D. T. Son and A. O. Starinets, Phys. Rev. Lett. **94**, 111601 (2005) [hep-th/0405231].

[45] M. Laine and Y. Schroder, Phys. Rev. D **73**, 085009 (2006) [hep-ph/0603048].

[46] P. F. Kolb and U. W. Heinz, In *Hwa, R.C. (ed.) et al.: Quark gluon plasma* 634-714 [nucl-th/0305084].

[47] M. Luzum, C. Gombeaud and J. Y. Ollitrault, Phys. Rev. C **81**, 054910 (2010) [arXiv:1004.2024 [nucl-th]].

[48] D. Teaney, Phys. Rev. C **68**, 034913 (2003) [nucl-th/0301099].

[49] K. Dusling, G. D. Moore and D. Teaney, Phys. Rev. C **81**, 034907 (2010) [arXiv:0909.0754 [nucl-th]].

[50] R. S. Bhalerao, A. Jaiswal, S. Pal and V. Sreekanth, Phys. Rev. C **89**, no. 5, 054903 (2014) [arXiv:1312.1864 [nucl-th]].

[51] M. Luzum and J. Y. Ollitrault, Phys. Rev. C **82**, 014906 (2010) [arXiv:1004.2023 [nucl-th]].

[52] A. Monnai and T. Hirano, Phys. Rev. C **80**, 054906 (2009) [arXiv:0903.4436 [nucl-th]].

[53] P. Bozek, Phys. Rev. C **81**, 034909 (2010) [arXiv:0911.2397 [nucl-th]].

[54] K. Dusling and T. Schfer, Phys. Rev. C **85**, 044909 (2012) [arXiv:1109.5181 [hep-ph]].

[55] J. Noronha-Hostler, G. S. Denicol, J. Noronha, R. P. G. Andrade and F. Grassi, Phys. Rev. C **88**, 044916 (2013) [arXiv:1305.1981 [nucl-th]].

[56] C. Adler *et al.* [STAR Collaboration], Phys. Rev. C **66**, 034904 (2002) [nucl-ex/0206001].

[57] S. S. Adler *et al.* [PHENIX Collaboration], Phys. Rev. Lett. **91**, 182301 (2003) [nucl-ex/0305013].

[58] M. Luzum, Phys. Lett. B **696**, 499 (2011) [arXiv:1011.5773 [nucl-th]].

[59] A. M. Poskanzer and S. A. Voloshin, Phys. Rev. C **58**, 1671 (1998) [nucl-ex/9805001].